INTERNAL REPORT

Design, Fabrication and Characterization of a Low-Pass Filter for the IF section of the Sardinia Radio Telescope

Simone Dessì, Giuseppe Valente

Report N. 38,
released: 08 Agosto 2014

Reviewer: Tonino Pisanu

Osservatorio
Astronomico
di Cagliari

Sommario

1.0 Introduction

Most communication systems contain an RF front end which performs signal processing with RF filters. Microstrip filters are a low cost means of doing this. There is an increasing demand for microwave and millimeter-wave systems to meet the emerging telecommunication challenges with respect to size, performance and cost. Conventional microstrip low pass filters, such as LC-ladder type filter using stepped-impedance transmission line or open-circuited stubs, have been widely used in microwave systems. To obtain an even sharper rate of cutoff for a given number of reactive elements, filters with elliptic function response are often desired, which can give infinite attenuation poles at finite frequency. One way to obtain them is to make use of stepped-impedance lines shunted to the main transmission line to approximate the L-C elements shunted along a transmission line. Microstrip line is a good candidate for filter design due to its advantages of low cost, compact size, light weight, planar structure and easy integration with other components on a single board.

In our specific situation, the fabricated filter will be inserted into the following receiver chain

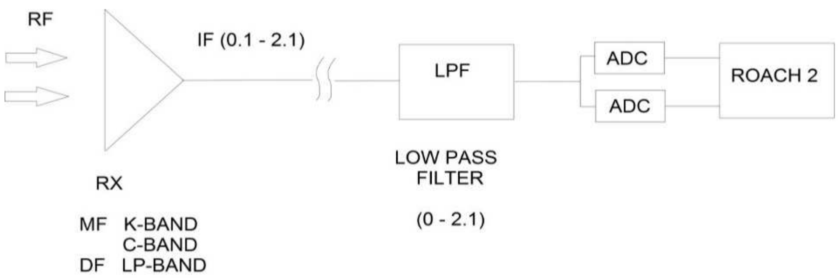

Figure 1. Generic scheme of the RF receiver chain in Sardinia Radio Telescope.

where the ROACH-2 block (Reconfigurable Open Architecture Computing Hardware) is a stand-alone FPGA board and is the successor to the original ROACH board; as seen in the above figure, it is connected to the AD converters (to turn an analog signal into a stream of digital data) and its frequency is f_c=5 Gsample/s (and, in agreement with the Nyquist theorem, B_{max}=2.5 GHz). This last is a high value for the characteristics of the ROACH-2 block and, as a result, it is necessary to decrease it to save bandwidth, cutting off the band without information and considering the only useful band. To do this, a low pass filter with a cutoff frequency of about 2 GHz should be inserted within the above chain. In this way, the B_{max} value (and the corresponding frequency) will decrease, in agreement with the operating characteristics of the Roach-2. Here three low pass filters were designed and simulated on the FR-4 substrate 1.6 mm in thickness and with a relative dielectric constant of 4.4. FR-4 has been chosen for this study because of its low cost and convenient availability, hence can be used for microstrip filter prototyping. The design and simulations are performed using the Sonnet EM Simulator and the design procedure is verified by comparing with analysis results. The specifications for the filters under consideration are:

Relative Dielectric Constant ε_r	4.4
Height of substrate h	1.6 mm
Cutoff frequency @ 3dB	2.1 GHz
The loss tangent tanδ	0.02
Rejection L_{AS}@ 2.2GHz	<-30dB (or-25dB)
Return Loss LR	<15
Metallization thickness	0.035 mm

2.0 Filter design method

The design of low pass filters involves two main steps. The first one is to select an appropriate low pass prototype. The choice of the type of response, including pass band ripple and the number of reactive elements (order of the filter) will depend on the required specifications. The element values of the low pass prototype filters, which are usually normalized to make a source impedance g_0=1 and a cutoff frequency Ω_c=1, are then transformed to the L-C elements for the desired cutoff frequency and the desired source impedance, which is normally 50Ω for microstrip filters. The next main step in the design of microstrip low pass filters is to find an appropriate realization that approximates the lumped element filter. It has been assumed, under the condition $Z_{low} < Z_0 < Z_{high}$:

- the filter impedance Z_0 = 50 Ω
- the highest line impedance Z_{high} = Z_L = 122 Ω
- the lowest line impedance Z_{low}= Zc = 26 Ω

3.0 Stepped-Impedance low pass filter

The minimum return loss LR or the maximum voltage standing wave ratio *VSWR* in the pass-band is specified instead of the pass-band ripple L_{AR}. If the return loss is defined by

$$LR(\Omega) = 10 \log[1 - |S21(j\Omega)|^2] dB$$

and the minimum pass band return loss is LR dB (LR < 0), the corresponding pass-band ripple is

$$L_{AR} = -10 \log(1 - 10^{0.1\, LR})\ dB$$

therefore, for LR=15dB, L_{AR}=0.139dB.

For the required pass-band ripple L_{AR} dB and the minimum stop-band attenuation L_{AS} dB, the degree of a Chebyshev low-pass prototype, which will meet these specification, can be found by

$$n = \frac{cosh^{-1}\sqrt{\frac{10^{0.1\, L_{AS}} - 1}{10^{0.1\, L_{AR}} - 1}}}{cosh^{-1}\ \Omega_s}$$

Where $\Omega s = \frac{fs}{fc} = \frac{2.2}{2.1} = 1.05$

In this case the order calculated is n=19, a very high value of section lines. To decrease the filter order it is necessary to consider the variation of the parameters LR, L_{AS}, fs; the most significant results in the study were examined with the creation of charts and graphs using Excel software: a good choice is to use the compromise with LR=12dB (therefore L_{AR}=0.2dB), L_{AS}=26dB, fs=2.25GHz, fc =2.05GHz, to obtain n=13.
Fig. 2(a) shows a general structure of the stepped-impedance low pass microstrip filters, which use a cascaded structure of alternating high- and low impedance transmission lines. The high-impedance lines act as series inductors and the low-impedance lines act as shunt capacitors. Therefore, this filter structure is directly realizing the L-C ladder type of low pass filters of Fig. 2(b).

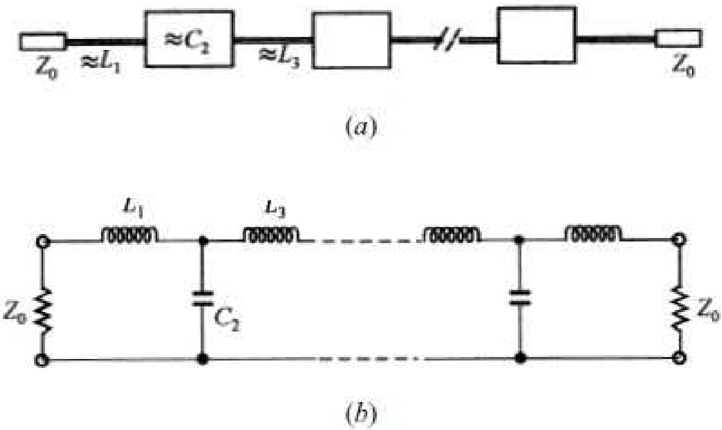

Figure 2. General structure of the stepped-impedance low pass microstrip filters (a); L-C ladder type of low pass filters to be approximated (b).

A low-pass prototype with Chebyshev response is chosen, whose element values are, for n=13 and pass-band ripple L_{AR}=0.2dB:

$g_0=g_{14}$	$g_1=g_{13}$	$g_2=g_{12}$	$g_3=g_{11}$	$g_4=g_{10}$	$g_5=g_9$	$g_6=g_8$	g_7
1	1.3972	1.4059	2.3323	1.5532	2.4140	1.5758	2.4276

Table 1. Chebyshev coefficients.

Using the element transformations

$L_i=\left(\frac{Z0\ \omega 0}{2\pi fc\ g0}\right)g_i$, $C_j=\left(\frac{g0\ \omega 0}{Z0\ 2\pi fc}\right)g_j$ for i=1, 3, 5…, j=2, 4, 6…,

$L_1=L_{13}$	$C_2=C_{12}$	$L_3=L_{11}$	$C_4=C_{10}$	$L_5=L_9$	$C_6=C$	L_7
5.43nH	2.18pF	9.06nH	2.41pF	9.37nH	2.45pF	9.43nH

Table 2. Inductance and capacitance values.

The filter was fabricated on a FR-4 substrate with a relative dielectric constant of 4.4 and a thickness of 1.6mm. The relevant design parameters of microstrip lines are given by:

- $Z_{low}=Z_c=26\Omega$ $Z_c\sqrt{\varepsilon_r}<$ 89.91

$$\frac{W}{h}=\frac{2}{\pi}\{B-1-\ln(2B-1)+\frac{\varepsilon_r-1}{2\varepsilon_r}[\ln(B-1)+0.39-\frac{0.61}{\varepsilon_r}]\}$$

$B=\frac{60\ \pi^2}{Zc\sqrt{\varepsilon_r}}$ =10.85 therefore W_C=7.76 mm

The effective dielectric constant ε_{eff} is calculated based on the ratio of the width W of the transmission line and the height h of the substrate which in this design is h=1.6mm:

For $\frac{W}{h}\geq 1$ $\varepsilon_{effc}=\frac{\varepsilon_r+1}{2}+\frac{\varepsilon_r-1}{2}\left[\frac{1}{\sqrt{1+12\frac{h}{W}}}\right]$= 3.61

while the effective width is, for $\frac{W}{h} > 1$:

W_{ec}= W+[1.393+0.667 ln($\frac{W}{h}$ + 1.444)]h = 11.9 mm

- Z_0= 50Ω $\qquad$ $Z_0\sqrt{\varepsilon_r}$> 89.91

$\frac{W}{h} = \frac{8\exp(A)}{\exp(2A)-2}$ where $A=\frac{Z0}{60}\sqrt{\frac{\varepsilon_r+1}{2}} + \frac{\varepsilon_r-1}{\varepsilon_r+1}\left[0.23 + \frac{0.11}{\varepsilon_r}\right] = 1.52$

Therefore: W_0=3.1 mm

For $\frac{W}{h} \geq 1$ $\qquad$ $\varepsilon_{eff}= \frac{\varepsilon_r+1}{2} + \frac{\varepsilon_r-1}{2}\left[\frac{1}{\sqrt{1+12\frac{h}{W}}}\right]$= 3.33

$W_{e\,c}$ = W+[1.393+0.667 ln($\frac{W}{h}$ + 1.444)]h = 6.6 mm

- Z_{high}=Z_L=122Ω $\qquad$ $Z_L\sqrt{\varepsilon r}$> 89.91

$\frac{W}{h} = \frac{8\exp(A)}{\exp(2A)-2}$ where $A=\frac{ZL}{60}\sqrt{\frac{\varepsilon_r+1}{2}} + \frac{\varepsilon_r-1}{\varepsilon_r+1}\left[0.23 + \frac{0.11}{\varepsilon_r}\right] = 3.49$

Therefore W_L=0.38 mm

For $\frac{W}{h} < 1$ $\qquad$ $\varepsilon_{effL} = \frac{\varepsilon_r+1}{2} + \frac{\varepsilon_r-1}{2}\left[\frac{1}{\sqrt{1+12\frac{h}{W}}} + 0.04(1-\frac{W}{h})^2\right]$= 2.97

$$W_{e\,L} = \frac{2\pi\, h}{\ln[\frac{8h}{W}+\frac{W}{4h}]} = 2.86 \text{ mm}$$

The relevant design parameters of microstrip lines are listed in table 3.

Characteristic impedance [Ω]	Z_C=26	Z_0=50	Z_L=122
Microstrip line widths [mm]	W_C=7.76	W_0=3.1	W_L=0.38

Table 3. Relevant design parameters of microstrip lines.

Initial physical lengths of the high and low impedance lines for realization of the desired L-C elements can be determined considering

$$l_{Li} = \frac{\lambda}{2\pi}\left(\frac{\omega cLi}{Zl}\right) \qquad l_{Ci} = \frac{\lambda}{2\pi}(\omega cCiZc)$$

Where the wavelength λ is connected to the dielectric constant of the substrate:

$$\lambda = \frac{c_0}{\sqrt{\varepsilon_r f}} = \frac{3x10^8}{\sqrt{4.4}\, x\ 2.05x10^9} = 0.069 \text{ m}$$

To meet initial specifications, it has been used an iterative method of gradual optimization, maintaining the widths unchanged and acting on the only inductive and capacitive lengths, to obtain the final dimensions of the circuit (Table 4).

Calculated Section [mm]	**Optimized Section [mm]**	**Z_{high} or Z_{low} [Ω]**	**W_i [mm]**
$l_{L1}=l_{L13=}6.3$	$l_{L1}= l_{L13} = 6.76$	122	0.38
$l_{C2}=l_{C12=}8$	$l_{C2} =l_{C12} = 7.14$	26	7.76
$l_{L3}=l_{L11=}10.5$	$l_{L3} = l_{L11} = 11.02$	122	0.38
$l_{C4}=l_{C10=}$ 8.8	$l_{C4} = l_{C10} = 7.94$	26	7.76
$l_{L5}=l_{L9=}10.8$	$l_{L5} = l_{L9} = 11.32$	122	0.38
$l_{C6}=l_{C8=}9$	$l_{C6} = l_{C8} = 8.14$	26	7.76
$l_{L7=}10.9$	$l_{L7} = 11.34$	122	0.38
$l_{50\Omega} = 10$	$l_{50\Omega} = 10$	50	3.1

Table 4. Calculated and optimized dimensions of the Stepped-Impedance Low Pass Filter.

3.1 Simulation and measured results

The design is verified with the Sonnet EM Simulation, a full-wave analysis engine which takes into account all possible coupling mechanisms. The layout of the microstrip filter with the final design dimensions is given in Fig. 3, the fabricated filter is illustrated in Fig.4 while the simulated (using Sonnet) and measured (using Vector Network Analyzer) frequency response is given in Fig.5.

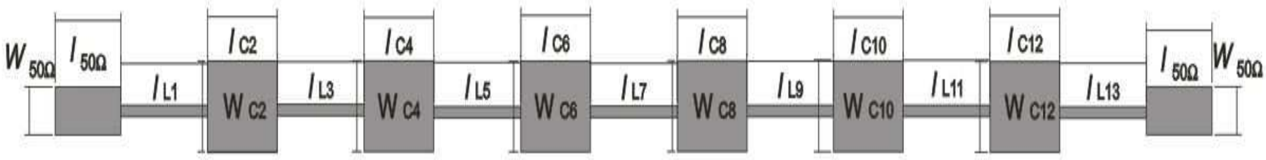

Figure 3. Layout of a 13-pole Stepped-Impedance Microstrip Low Pass Filter on a FR-4 substrate with ε_r = 4.4 and h=1.6mm.

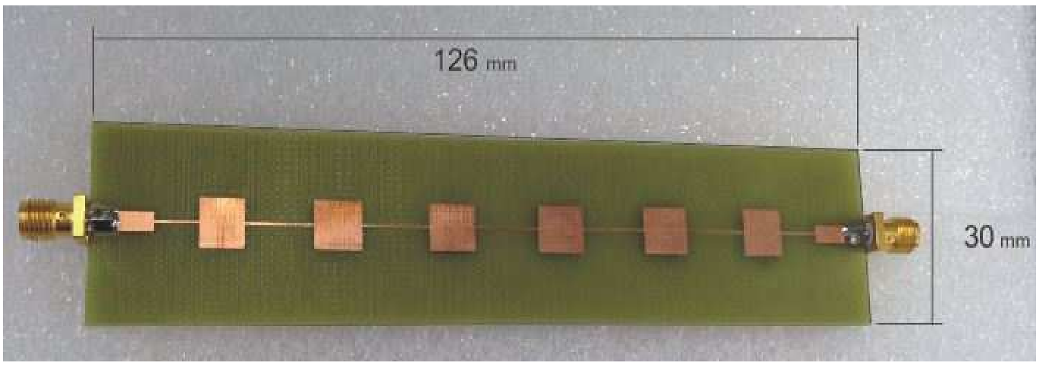

Figure 4. Layout of the Fabricated 13-pole Stepped-Impedance microstrip Low Pass Filter on a FR-4 substrate with εr =4.4 and h=1.6mm.

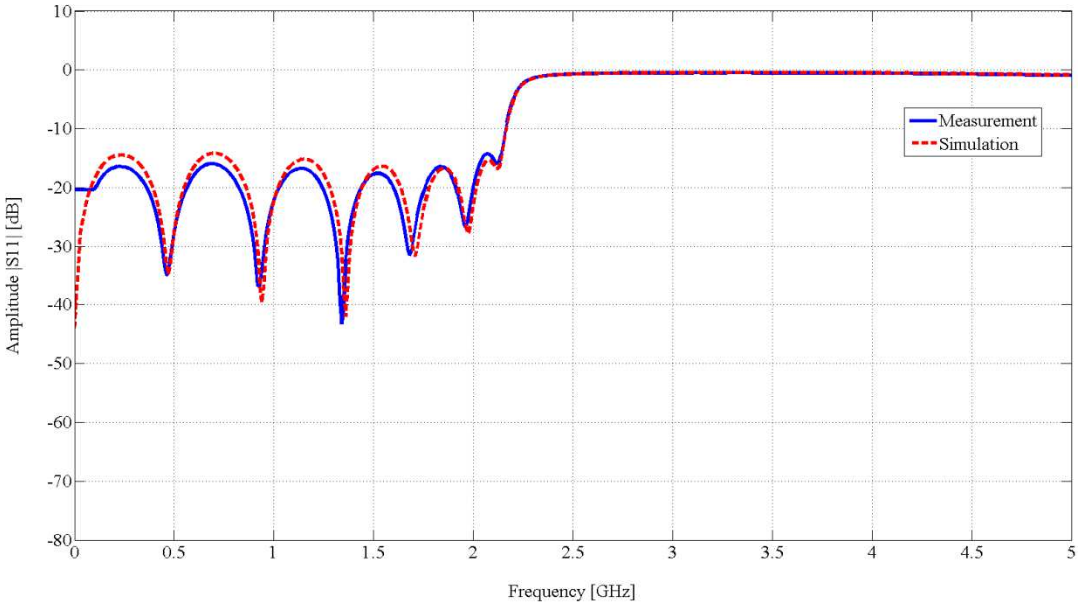

(a)

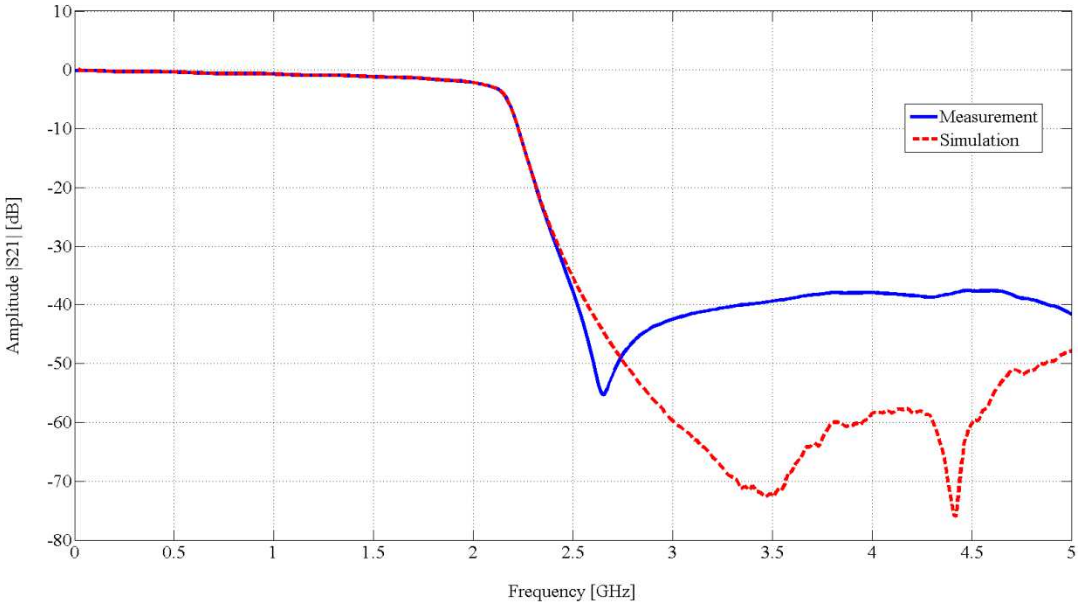

(b)

Figure 5. Simulated (dashed line) and measured (continuous line) frequency response of the Stepped-Impedance Low Pass Filter: (a) S_{11} parameters, (b) S_{21} parameters.

3.2 Considerations

A Stepped-Impedance low pass microstrip filter has been simulated, designed, fabricated and tested by measurement using a ROHDE&SCHWARZ ZVA 67 Vector Network Analyzer and the ZV-Z218 calibration kit. The measured values are very similar to the simulated values; from Fig. 5 it is evident that the two Return Loss are very similar and lower than -15dB.The simulated cutoff frequency achieved is the same of the design specification value (2.05 GHz) but the measured one is greater (2.1 GHz); the simulated Insertion Loss at 2.25 GHz is -16dB while the measured one is -13dB. The discrepancy can be corrected using a different dielectric constant ($\mathcal{E}_r$=4.3) and further optimizing the capacitive and inductive lenghts with small successive corrections. In this way can be obtained an excellent agreement with the initial specifications.

4.0 Open-circuited stubs low pass filter

The previous stepped-impedance low pass filter realizes the shunt capacitors of the low pass prototype as low impedance lines in the transmission path.
An alternative realization of a shunt capacitor is to use an open-circuited stub. For comparison, the same prototype filter and the substrate of the previous design example of stepped-impedance microstrip low pass filter has been employed. Also, the same high-impedance (Z_{high}=122 Ω) lines are used for the series inductors, while the open-circuited stub will have the same low characteristic impedance as Z_{low}=26 Ω. Thus, the design parameters of the microstrip lines listed in Table 3 are valid for this design example. To realize the lumped L-C elements, the physical lengths of the high-impedance lines and the open-circuited stubs are initially determined by

$$l_{Li} = \frac{\lambda}{2\pi}\left(\frac{\omega c Li}{Zl}\right) \qquad\qquad l_{Ci} = \frac{\lambda}{2\pi}(\omega c Ci Zc)$$

To correct for the fringing capacitance at the ends of the line elements for C_2, C_4 and C_6, the open-end effect is calculated using the equation

$$\frac{\Delta l}{h} = 0.412\,\frac{\mathcal{E}_e+0.3}{\mathcal{E}_e-0.258}\,\frac{\frac{W}{h}+0.264}{\frac{W}{h}+0.8} \qquad\qquad \Delta l = 0.69 \text{ mm}$$

Where $\mathcal{E}_e$ and W are respectively the effective dielectric constant and the width of the capacitor. We need to subtract Δl from the above-determined l_{C2}, l_{C4}, l_{C6}, which gives l_{C2}=7.31mm, l_{C4}=8.11mm, l_{C6}=8.31 mm. To meet initial specifications, capacitive and inductive lengths have been consequently optimized with the same technique used for the optimization of the Stepped-Impedance filter; the final dimensions of the circuit are listed in the following table:

Calculated Section [mm]	Optimized Section [mm]	Z_{high} or Z_{low} [Ω]	W_i [mm]
$l_{L1}=l_{L13}$ = 6.30	$l_{L1}=l_{L13}$ = 6.30	122	0.38
$l_{C2}=l_{C12}$ = 8.00	$l_{C2}=l_{C12}$ = 6.60	26	7.76
$l_{L3}=l_{L11}$=10.50	$l_{L3}=l_{L11}$=10.50	122	0.38
$l_{C4}=l_{C10}$ =8.80	$l_{C4}=l_{C10}$ =7.40	26	7.76
$l_{L5}=l_{L9}$=10.80	$l_{L5}=l_{L9}$=10.80	122	0.38
$l_{C6}=l_{C8}$=9.00	$l_{C6}=l_{C8}$=7.60	26	7.76
l_{L7}=10.90	l_{L7}=10.90	122	0.38
$l_{50\Omega}$=10	$l_{50\Omega}$=10	50	3.1

Table 5. Calculated and final dimensions of the Open-Circuited Stubs Low Pass Filter (for n=13).

4.1 Simulation and measured results

The design is verified with the Sonnet EM Simulation. The layout of the microstrip filter with the final design dimensions is shown in Fig. 6, the fabricated filter is shown in Fig. 7 while the comparison between simulated and measured frequency response of this microstrip filter is illustrated in Fig. 8.

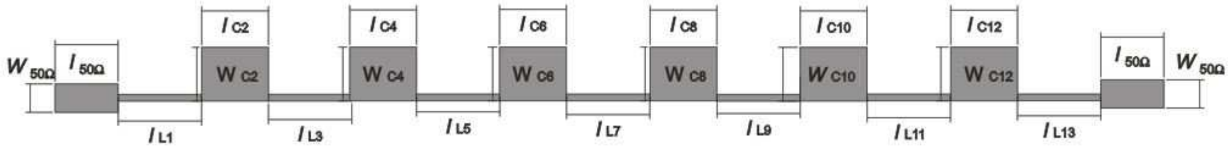

Figure 6. layout of a 13-pole Open Stubs Microstrip Low Pass Filter on a FR-4 substrate with $\varepsilon_r = 4.4$ and h=1.6 mm.

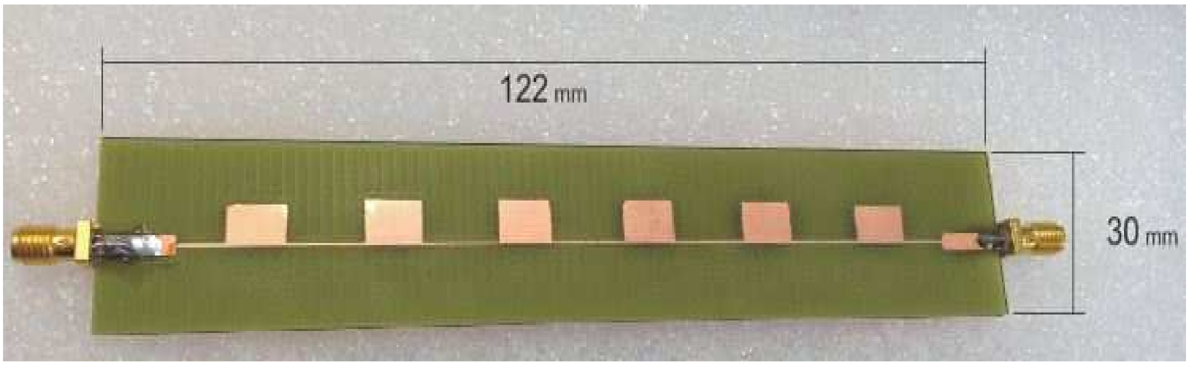

Figure 7. Layout of the Fabricated 13-pole Open-Stubs Microstrip Low Pass Filter on a FR-4 substrate with $\varepsilon_r = 4.4$ and h=1.6 mm.

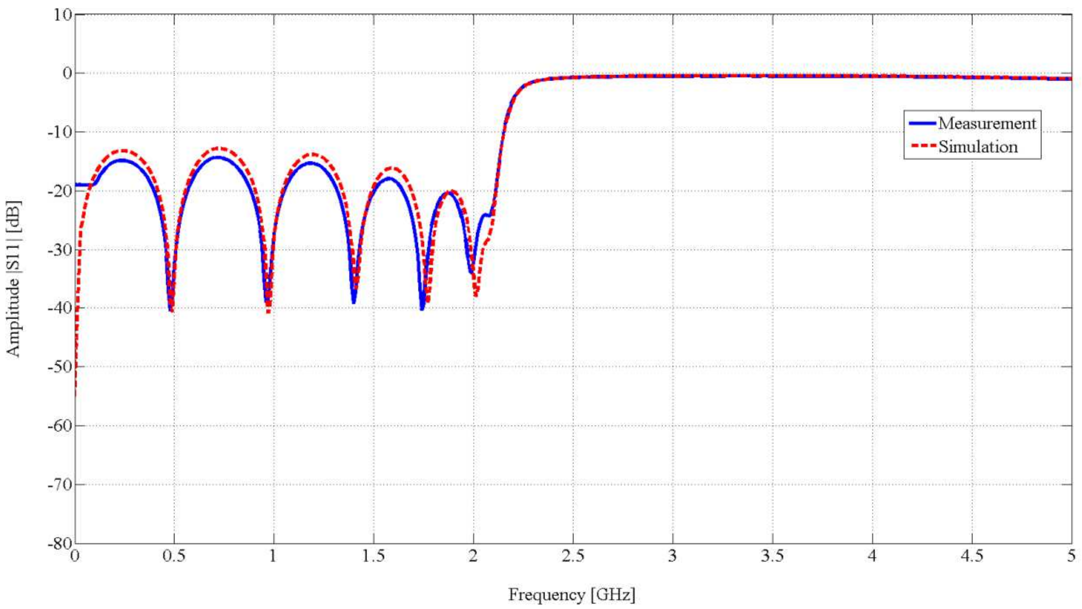

(a)

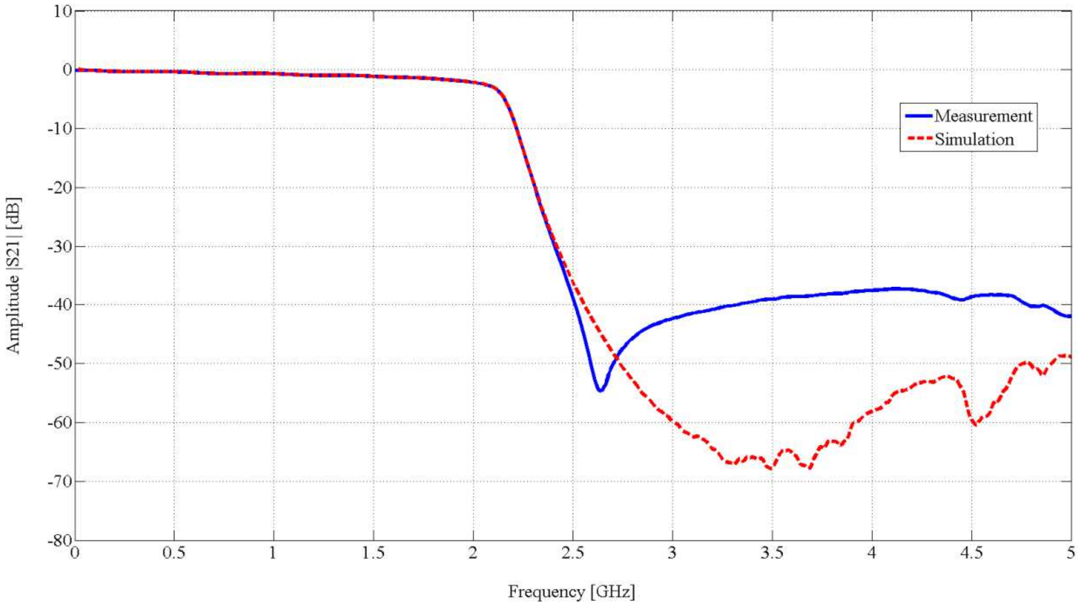

(b)

Figure 8. Simulated (dashed line) and measured (continuous line) frequency response of the Open Stubs Low Pass Filter: (a) S_{11} parameters, (b) S_{12} parameters.

4.2 Considerations

An Open Stubs low pass microstrip filter has been simulated, designed, fabricated and tested by measurement with the vector network analyzer. Compared to the stepped-impedance response, both filters show a very similar filtering characteristic in the given frequency range, as expected, as they are designed based on the same prototype filter. However, one should bear in mind that the two filters have different realizations that only approximate the lumped elements of the prototype near the cutoff frequency, and hence, their wide-band frequency responses can be different. From Fig. 8 it is evident that the two Return Loss are very similar and their value is -15dB. The achieved simulated cutoff frequency is the same of the design specification value (2.05 GHz) but the measured one is greater (2.1 GHz); the simulated Insertion Loss at 2.25 GHz is -19dB while the measured one is -14dB. The discrepancy can be corrected using a different dielectric constant($\mathcal{E}_r$=4.3) and further optimizing the capacitive and inductive lenghts with small successive corrections. In this way we can obtain an excellent agreement with the initial specifications. In conclusion, it has been shown that the Open Stubs filter has a greater selectivity than the Stepped-Impedance one, considering the same number of reactive elements.

5.0 Elliptic low pass filter

The filter is assumed to be fabricated on a FR-4 substrate of dielectric constant ε_r and of thickness h for angular normalized cutoff frequency, using the element transformation [2]. Fig. 9 illustrates two commonly used network structures for elliptic function low pass prototype filters. In Fig. 9(a), the series branches of parallel-resonant circuits are introduced for realizing the finite-frequency transmission zeros, since they block transmission by having infinite series impedance (open-circuit) at resonance. For this form of the elliptic function low pass prototype [Fig. 9(a)], g_i for odd *i* (*i* = 1, 3, · · ·) represent the capacitance of a shunt capacitor, g_i for even i (*i* = 2, 4, · · ·) represent the inductance of an inductor, and the primed g_i for even *i* (*i* = 2, 4, · · ·) are the capacitance of a capacitor in a series branch of parallel-resonant circuit. For the dual realization form in Fig. 9(b), the shunt branches of series-resonant circuits are used for implementing the finite-frequency transmission zeros, since they short out transmission at resonance. In this case, referring to Fig. 9(b), g_i for odd i(i = 1, 3, · · ·) are the inductance of a series inductor, g_i for even i (i = 2, 4, · · ·) are the capacitance of a capacitor, and primed g_i for even i (i = 2, 4, · · ·) indicate the inductance of an inductor in a shunt branch of series-resonant circuit. Again, either form may be used, because both give the same response [1].

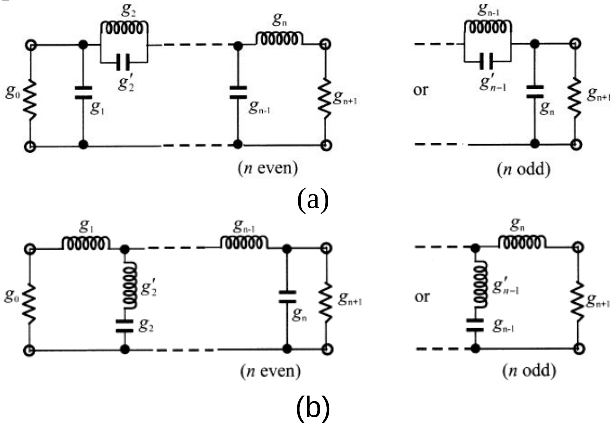

Figure 9. Low pass prototype filters for elliptic function filters with (a) series parallel-resonant branches, (b) its dual with shunt series-resonant branches.

The degree for an elliptic function low-pass prototype to meet a given specification may be found from design tables such as Table 3.3 [1]. For instance, considering L_{AS}=30dB at Ω_s=1.05 and the pass-band ripple L_{AR}=0.1dB, calculated by

$$L_{AR} = -10 \log(1 - 10^{0.1\,LR})\ \text{dB}$$

where LR=15dB, we can determine immediately n=7, which is the order of the elliptic filter. The element values for elliptic function low-pass prototype filters may be obtained from Table 3.3 [1]. For this design, we use the following low-pass prototype values:

$g_1=g_{L1}$	$g_2=g_{C2}$	$g_2'=g_{L2}$	$g_3=g_{L3}$	$g_4=g_{C4}$	$g_4'=g_{L4}$	$g_5=g_{L5}$	$g_6=g_{C6}$	$g_6'=g_{L6}$	$g_7=g_{L7}$
0.9194	1.0766	0.3422	1.0962	0.4052	2.2085	0.8434	0.5034	2.2085	0.4110

Table 6. Elliptic coefficients

The microstrip filter is designed to have a cutoff frequency fc=2.05 GHz and input/output terminal impedance Z_0=50Ω. Therefore, the L-C element values, which are scaled to Z_0 and fc, can be determined by

$$Li = \frac{1}{2\pi fc} Z_0\, g_{Li} \qquad Ci = \frac{g_{ci}}{2\pi fc Z_0}$$

L_1	L_2	L_3	L_4	L_5	L_6	L_7
3.57 nH	1.33 nH	4.26 nH	8.57 nH	3.27 nH	8.57 nH	1.59 nH
	C_2		C_4		C_6	
	1.67 pF		0.63 pF		0.78 pF	

Table 7. Inductance and capacitance values.

All inductors will be realized using high-impedance lines with characteristic impedance Z_{high}=122 Ω, whereas all the capacitors are realized using low-impedance lines with characteristic Z_{low}=26 Ω.

Initial physical lengths of the high and low impedance lines for realization of the desired L-C elements can be determined according to the design equations

$$l_{Li} = \frac{\lambda}{2\pi}\left(\frac{\omega c L i}{Z l}\right) \qquad\qquad l_{Ci} = \frac{\lambda}{2\pi}(\omega c C i Z c)$$

To correct for the fringing capacitance at the ends of the line elements for C_2, C_4 andC_6, the open-end effect is calculated using the equations presented in Chapter 4[1] and found to be Δl = 0.69 mm:

$$\frac{\Delta l}{h} = 0.412\,\frac{\varepsilon_e + 0.3}{\varepsilon_e - 0.258}\,\frac{\frac{W}{h} + 0.264}{\frac{W}{h} + 0.8}$$

Where$\varepsilon_e$and W are respectively the effective dielectric constant and the width of the capacitor. We need to subtract Δl from the above determined $l_{C2,}$ l_{C4}, l_{C6}, which gives l_{C2}=5.45 mm, l_{C4}=1.63 mm, l_{C6}=2.17 mm. Initial dimensions of the circuit lines don't meet the design specifications. Acting with an iterative method of gradual optimization on the only width of the three capacitors, which affect very specific frequency bands within the range of our interest (from 0 to 5GHz), it is possible to obtain the desired cut to the working frequency while maintaining a good slope and shape, to ensure an acceptable agreement with the design goals; it has been initially considered a not optimal accuracy of simulation to study separately the effect due to the three capacitors, observing the parameters variation of the scattering matrix. Once you get a configuration of widths to guarantee the desired cut, we consequently perform additional simulations considering a better accuracy. Again, acting on the only capacitive widths with small successive corrections, we obtained the optimized dimensions (Table 8).

Calculated Section [mm]	**Optimized Section [mm]**	**Z_{high} or Z_{low} [Ω]**	**W_i [mm]**
l_{L1} = 4.14	l_{L1} = 4.14	122	0.38
l_{C2} = 6.14	l_{C2} = 5.45	26	7.3
l_{L3} = 4.94	l_{L3} = 4.94	122	0.38
l_{C4} = 2.32	l_{C4} = 1.63	26	5
l_{L5} = 3.8	l_{L5} = 3.8	122	0.38
l_{C6} = 2.86	l_{C6} = 2.17	26	5
l_{L7} = 1.84	l_{L7} = 1.84	122	0.38
l_{L2} = 1.54	l_{L2} = 1.54	122	0.38
l_{L4} = 9.93	l_{L4} = 9.93	122	0.38
l_{L6} = 9.93	l_{L6} = 9.93	122	0.38
$l_{50\Omega}$ = 10	$l_{50\Omega}$ = 10	50	3.1

Table 8. Calculated and optimized dimensions of the Elliptic Low Pass Filter (for n=7).

5.1 Simulation and measured results with Ɛr=4.4

The design is verified with the Sonnet EM Simulation. The layout of the microstrip filter with the final design dimensions, for a dielectric constant of 4.4, is given in Fig. 10 and the simulated and measured frequency responses of this microstrip filter are illustrated in Fig. 11.

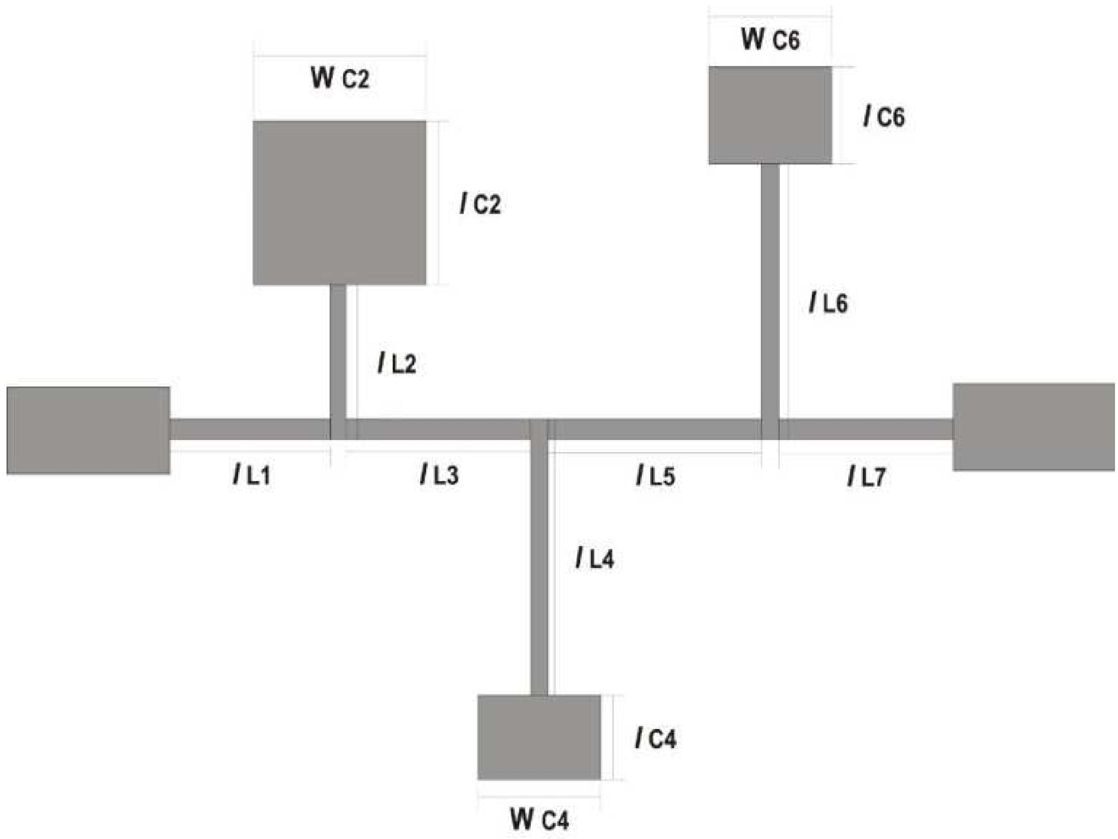

Figure 10. Layout of a 7-pole Elliptic Microstrip Low Pass Filter on a FR-4 substrate with $\varepsilon_r = 4.4$ and h=1.6mm at 2.05 GHz.

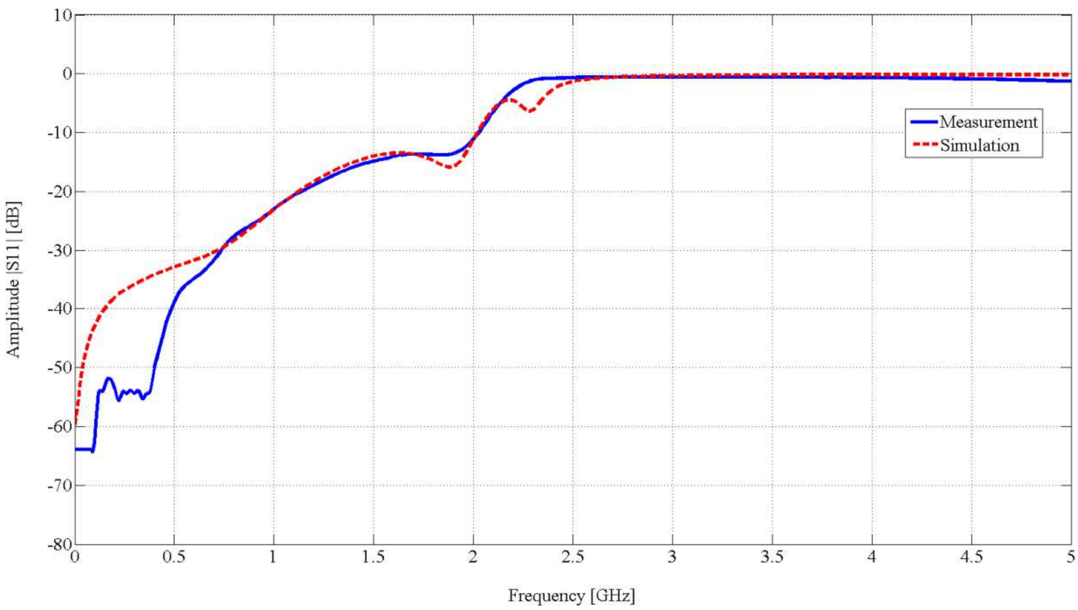

(a)

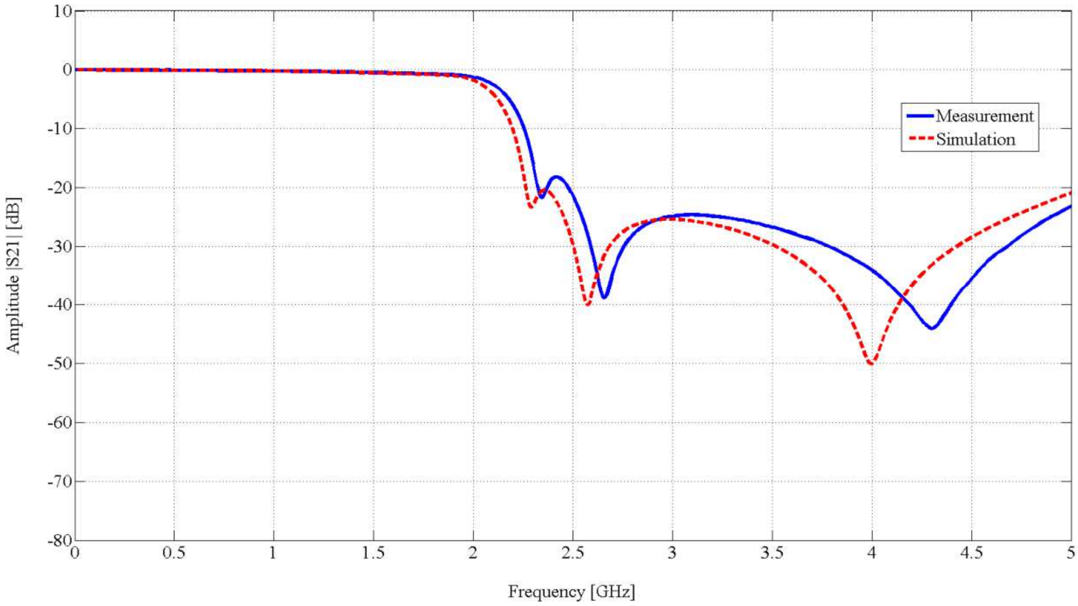

(b)

Figure 11. Simulated (dashed line) and measured (continuous line) frequency response of the Elliptic Low Pass Filter: (a) S_{11} parameters, (b) S_{12} parameters.

The results show a good agreement with the requirements but there's a small discrepancy between simulated and measured frequency responses; to correct this one it has been consequently optimized the capacitive widths using the same iterative method, considering a different dielectric constant Ɛr=4.3.

Section $l_{i\,[mm]}$	Z_{high} or $Z_{low\,[\Omega]}$	$W_{i[mm]}$
l_{L1} = 4.14	122	0.38
l_{C2} = 5.45	26	7.35
l_{L3} = 4.94	122	0.38
l_{C4} = 1.63	26	5.47
l_{L5} = 3.8	122	0.38
l_{C6} = 2.17	26	5.47
l_{L7} = 1.84	122	0.38
l_{L2} = 1.54	122	0.38
l_{L4} = 9.93	122	0.38
l_{L6} = 9.93	122	0.38
$l_{50\Omega}$ = 10	50	3.1

Table 9. Optimized Dimensions of the Elliptic Low Pass Filter with ε_r=4.3.

5.2 Simulation and measured results with Ɛr=4.3

The layout of the microstrip filter is the same of Fig. 10 and new dimensions are given in Table 9. Simulated and measured frequency responses of this microstrip filter are illustrated in Fig.12. The realized filter is shown in Fig. 13.

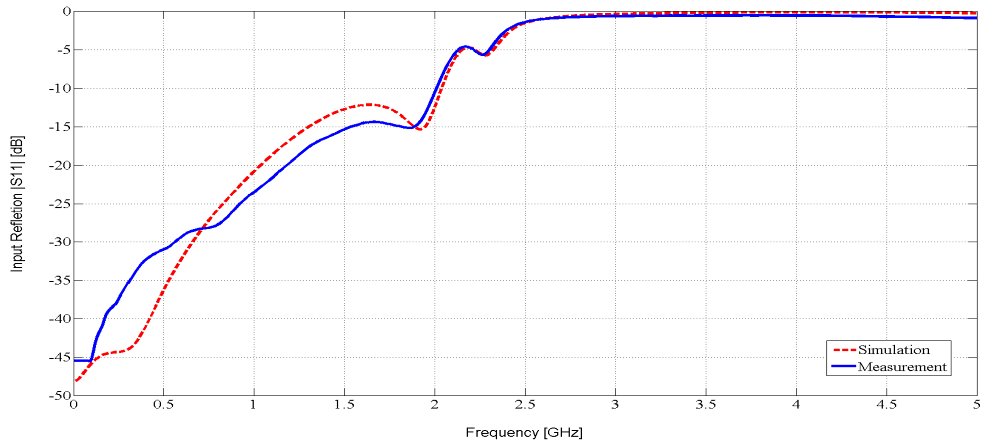

(a)

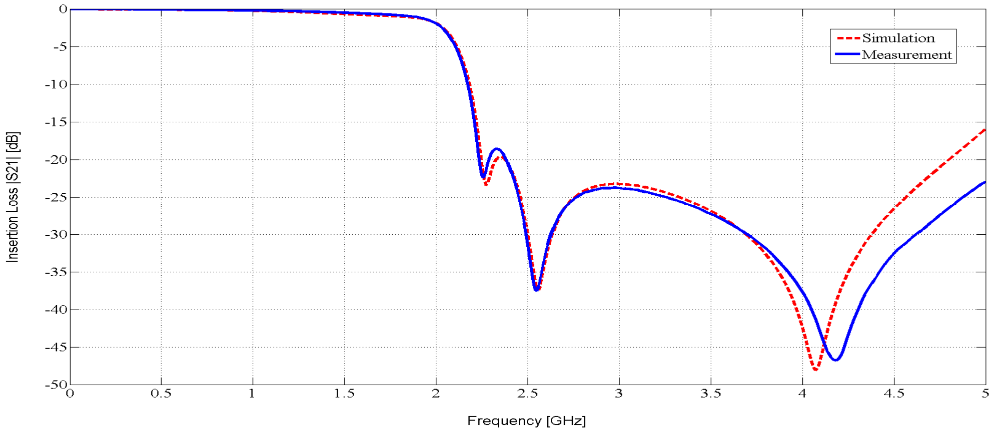

(b)

Figure 12. Comparison of simulated (dashed line) and measured (continuous line) performance for the Elliptic Low Pass Filter n=7 on FR-4 substrate, (a) S_{11} parameters, (b) S_{21} parameters.

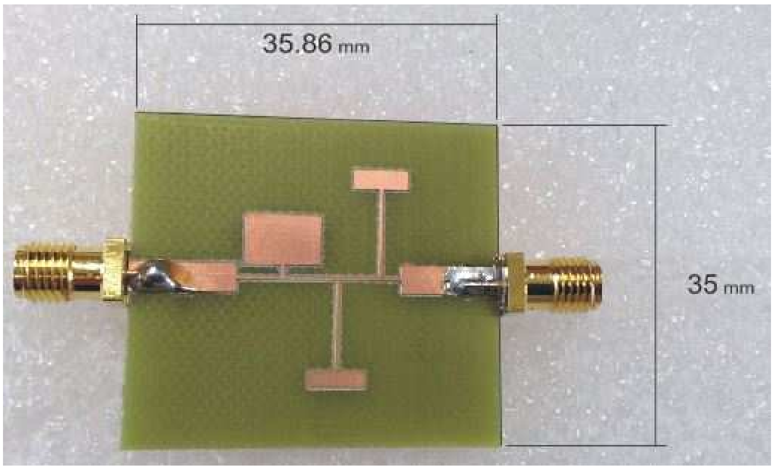

Figure 13. Layout of the Fabricated 7-pole Elliptic Microstrip Low Pass Filter on a Fr-4 substrate.

5.3 Considerations

Fig. 12 presents the comparison of the input reflection (S_{11}) and the insertion loss (S_{21}) obtained with the Sonnet EM simulation and the measured results for the prototype filter designed on Fr-4 substrate with an Ɛr=4.3; it is clear that the achieved result are in excellent agreement with the requirements; the curves overlap very well, showing the same cutoff frequency (2.05 GHz) and a small difference at 2.25 GHz: the simulated gain is -19.2 dB while the measured one is -21 dB. The Elliptic Low Pass Filter could be used in wireless applications and for the IF section of the Sardinia Radio Telescope, with significant simplification and cost reduction.

6.0 Mechanical design of the box

The software Autodesk Inventor Professional has been used to study the mechanical design of the box in which to insert the fabricated elliptic filter. The three parts which form the final assembly are: the box, the cap box and connectors. It was also created, with the same procedure, a box for the stepped impedance (Fig. 18) and for the open-circuited stubs filters but, in this section, we only show the design of the box for the elliptic filter. For the project it has been chosen the SMA R125.414.000 connector from Radiall [3]. The elliptic filter sizes are 35.86x35 mm (with a thickness of 1.56 mm); obviously, the box size will be larger than the filter, therefore it has been chosen a size of 47.86x47 mm. After choosing the reference plane, we designed the dimensions taking into account the data sheet.

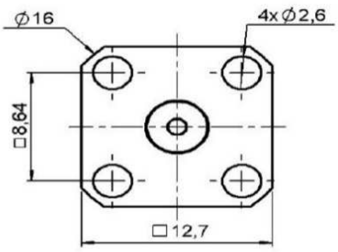

Figure 14. Front panel of connector R125.414.000

From the datasheet, 2.6 mm is the diameter of the side holes while 4.2 mm is the diameter of the central hole; the horizontal and vertical distance between the four side holes is 8.64 mm while the distances between them and the central hole is 4.32 mm.

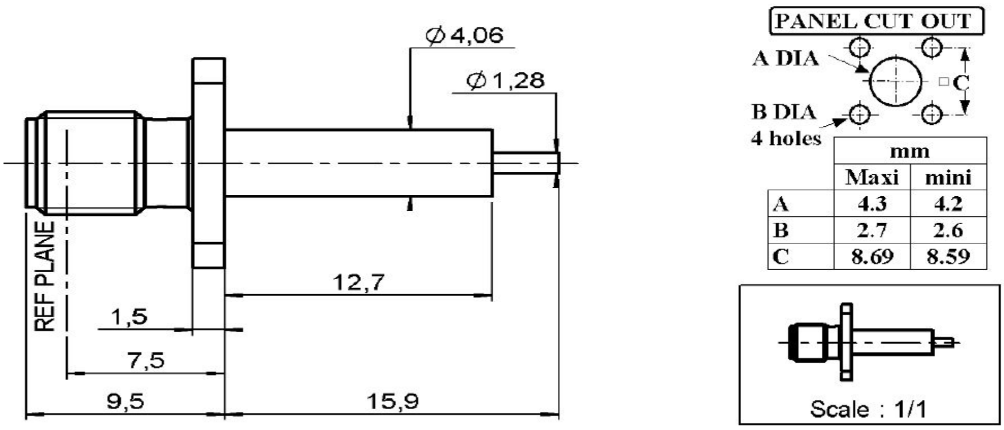

Figure 15. Drawing and quote of the connector R125.414.000

The distance between the central hole and the bottom wall is calculated considering d=1.28 mm and its value is given by (d/2)+(filter thickness)+(extrusion)=0.64+1.56+10=12.2 mm. The distance between the central hole and the side wall is given by 47/2=23.5 mm. After calculating the distances, it is necessary to impose the constraints of horizontality and verticality. The holes were built considering the use of screws with an ISO metric profile (for the side threaded holes) and with a simple profile (for the central one). The next step is the arrangement of the holes on the top edge for the cap: in this case, it is necessary the build of only four holes (because the elliptic filter has small sizes) spaced suitably; the cap has a dimension of 47.86x47 mm, it has 3 mm thick and four holes. The SMA connector is a separate part of the final assembly, and its dimensions (calculated considering the data sheet) are shown in Fig. 16.

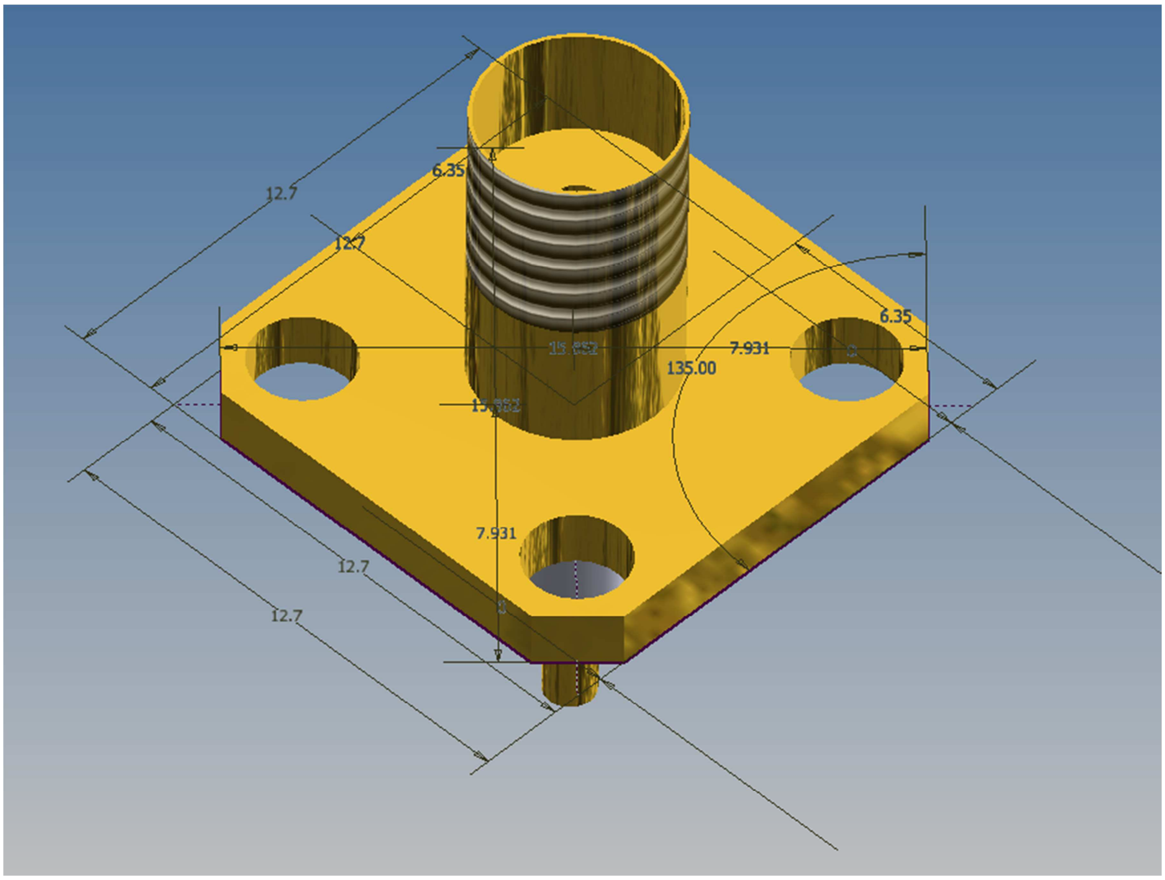

Figure 16. Designed connector R125.414.000

Finally, the three different parts have been assembled to obtain the final box (Fig. 17).

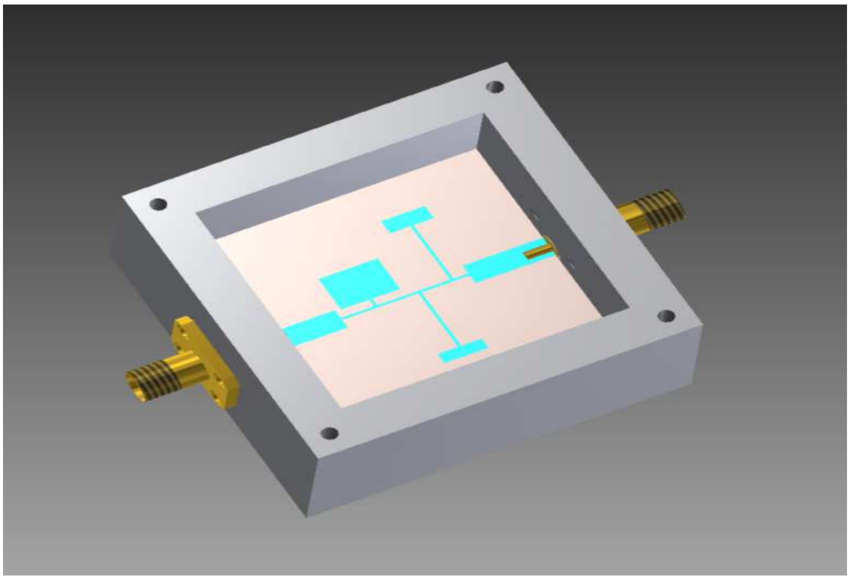

Figure 17. Final box for the Elliptic Low Pass Filter.

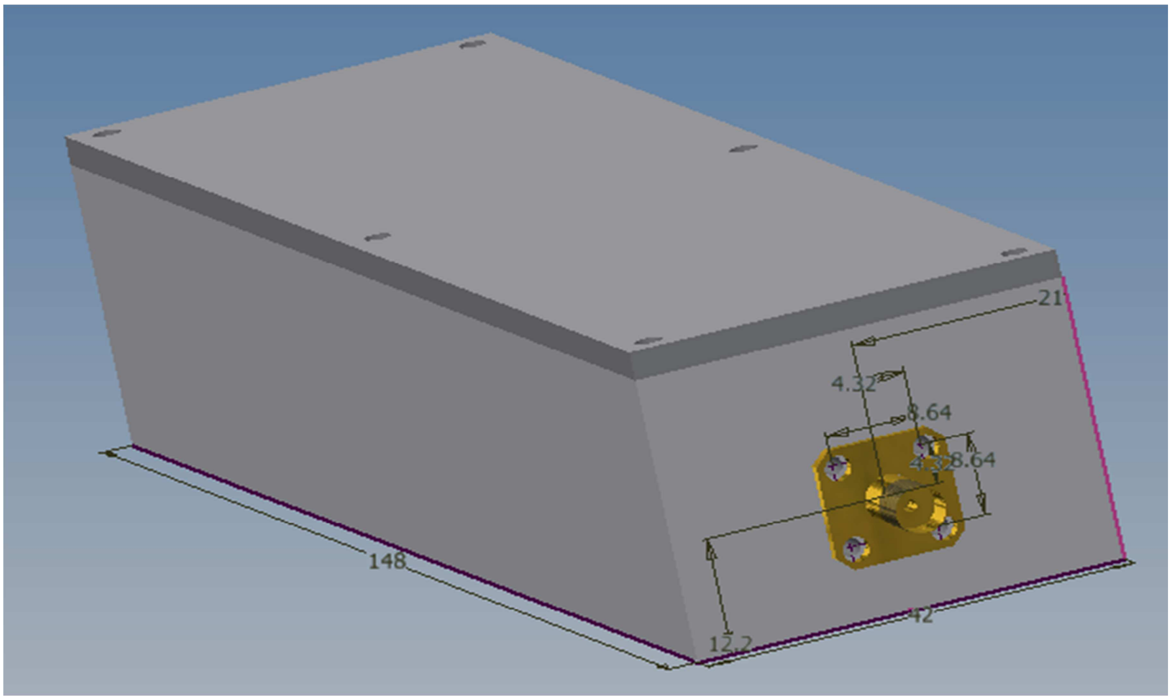

Figure 18. Final box for the Stepped-Impedance Low Pass Filter.

7.0 Conclusions

In this paper three different microstrip low pass filters on Fr-4 substrate were fabricated using the LPKF Printed Circuit Board prototyping machine and their parameters were measured using the ROHDE&SCHWARZ ZVA 67 Vector Network Analyzer (with the ZV-Z218 calibration kit). The numerical simulation and measurement of the fabricated filters, prove the validity of the analysis and design. In particular, regarding the most compact Elliptic Low Pass Filter, the achieved result show an excellent agreement with the specifications; it could be used for wireless communications (and WiMAX) and personal communication networks, because they have led to specific demands of miniaturization, portability, low-manufacturing cost and high performance in RF and millimeter-wave wireless systems [4]. Regarding WiMAX technology, its use is very frequent because it is necessary a channel selection filter with variable bandwidth [5]. The fabricated Elliptic Low Pass Filter could be also used in the IF section of the Sardinia Radio Telescope, with significant simplification and cost reduction.

8.0 Acknowledgments

I gratefully acknowledge G. Valente for his generous assistance, provided during my internship. I also thank E. Urru, A. Ladu and M. Pili for their help during the realization of the circuitries and of the box.

9.0 References

[1] JiaShen G.Hong, M.J.Lancaster, "Microstrip Filters for RF/Microwave Applications", John Wiley &Sons Inc., 2001.
[2] D.M.Pozar, "Microwave Engineering", John Wiley, 2000.
[3] Radiall - Innovator of Interconnect Components & More - www.radiall.com.
[4] H.H. Meinel, "Commercial Applications of Millimeter waves History, Present Status, and Future Trends," IEEE Trans. Microwave Theory and Tech., vol. 43, no. 7, pp. 1639-1653, July 1995.
[5] D.R. Huang, S.W. Kao, and Y.H. Pang, "A WiMAX receiver with variable bandwidth of 2.5–20 MHz and 93 dB Dynamic Gain Range in 0.13-μm CMOS Process", in Proc. IEEE RFIC Symp. Dig. Tech. Papers, Jun. 2007, pp. 369–372.